
Faster Repeated Evasion Attacks in Tree Ensembles

Lorenzo Cascioli¹ Laurens Devos¹ Ondřej Kuželka² Jesse Davis¹

Abstract

Tree ensembles are one of the most widely used model classes. However, these models are susceptible to adversarial examples, i.e., slightly perturbed examples that elicit a misprediction. There has been significant research on designing approaches to construct such examples for tree ensembles. But this is a computationally challenging problem that often must be solved a large number of times (e.g., for all examples in a training set). This is compounded by the fact that current approaches attempt to find such examples from scratch. In contrast, we exploit the fact that multiple similar problems are being solved. Specifically, our approach exploits the insight that adversarial examples for tree ensembles tend to perturb a consistent but relatively small set of features. We show that we can quickly identify this set of features and use this knowledge to speedup constructing adversarial examples.

1. Introduction

One of most popular and widely used class of models is tree ensembles which encompasses techniques such as gradient boosting (Friedman, 2001) and random forests (Breiman, 2001). However, like other flexible model classes such as (deep) neural networks (Szegedy et al., 2013; Goodfellow et al., 2014), they are susceptible to evasion attacks (Kantchelian et al., 2016). That is, an adversary can craft an imperceptible perturbation that, when applied to an otherwise valid input example, elicits a misprediction by the ensemble. There is significant interest in reasoning about tree ensembles to both generate such adversarial examples (Einzigler et al., 2019; Zhang et al., 2020) and perform empirical robustness checking (Kantchelian et al., 2016; Chen et al., 2019b; Devos et al., 2021a) where the goal is to determine how close the nearest adversarial example is.

Generating adversarial examples is an NP-hard problem (Kantchelian et al., 2016), which has spurred the de-

velopment of approximate techniques (Chen et al., 2019b; Zhang et al., 2020; Devos et al., 2021a). These methods exploit the structure of the trees to find adversarial examples faster, for example, by using graph transformations (Chen et al., 2019b) or discrete (heuristic) search (Zhang et al., 2020; Devos et al., 2021a; 2024). Still, these techniques can be slow, particularly if there is a large number of attributes in the domain. This is compounded by the fact that one often wants to generate large sets of adversarial examples.

A weakness to existing approaches is that they ignore the fact that adversarial example generation is often a sequential task where multiple similar problems are being solved in a row. That is, one has access to a large number of “normal” examples each of which should be perturbed to elicit a misprediction. Alas, existing approaches treat each considered example in isolation and solve the problem from scratch. However, there are likely regularities among the problems, meaning that the algorithms perform redundant work. If these regularities can be identified efficiently and this information can be exploited to guide the search for an adversarial example, then the run time performance of repeated adversarial example generation can be improved.

Studying these regularities in order to make adversarial example generation faster is an important problem. First, it advances our understanding of the nature of adversarial examples in tree ensembles and their generation methods. This might inspire improvements to generation methods, and in turn lead to better defense or detection methods. Second, model evaluation by verification (Ranzato & Zanella, 2020; Törnblom & Nadjm-Tehrani, 2020; Devos et al., 2021a) is quickly becoming important as machine learning is applied in sensitive application areas. Being able to efficiently generate adversarial examples is crucial in the computation of empirical robustness (e.g., (Devos et al., 2021a)), adversarial accuracy (e.g., (Vos & Verwer, 2021)), and for model hardening (e.g., (Kantchelian et al., 2016)).

We propose a novel approach that analyzes previously solved adversarial example generation tasks to inform the search for subsequent tasks. Our approach is based on the observation that for a fixed learned tree ensemble, adversarial examples tend to be generated by perturbing the same, relatively small set of features. We propose a theoretically grounded manner to quickly find this set of features. We

¹Department of Computer Science, KU Leuven, Leuven, Belgium ²Department of Computer Science, Czech Technical University, Prague, Czech Republic. Correspondence to: Lorenzo Cascioli <lorenzo.cascioli@kuleuven.be>.

propose two novel strategies to use the identified features to guide the search for adversarial examples, one of which is guaranteed to produce an adversarial example if it exists. We apply our proposed approach to two different algorithms for generating adversarial examples (Kantchelian et al., 2016; Devos et al., 2021a). Empirically, our approaches result in speedups of up to 35x and of 7.7x on average.

2. Preliminaries

We briefly explain tree ensembles, evasion attacks, and the two adversarial generation methods that we will use in the experiments. We assume a d -dimensional input space $\mathcal{X} \subseteq \mathbb{R}^d$ and binary output space $\mathcal{Y} = \{-1, 1\}$. We focus on binary classification because most existing methods for verifying or generating adversarial examples for tree ensembles are designed for this setting (Andriushchenko & Hein, 2019; Kantchelian et al., 2016; Devos et al., 2021a).

2.1. Tree Ensembles

Tree ensembles include popular algorithms such as (gradient) boosted decision trees (GBDTs) (Friedman, 2001) (e.g., XGBoost (Chen & Guestrin, 2016)) and random forests (Breiman, 2001) (e.g., as in scikit-learn (Pedregosa et al., 2011)). A tree ensemble contains a number of trees and most implementations only learn binary trees. A binary tree T contains two types of nodes. *Internal nodes* store references to a left and a right sub-tree, and a split condition on some attribute f in the form of a less-than comparison $X_f < \tau$, where τ is the split value. *Leaf nodes* have no children and only contain an output value. Each tree starts with a *root node*, the only one without a parent.

Given an example x , an individual tree is evaluated recursively starting from the *root node*. In each internal node, the split condition is applied and if it is satisfied, then the example is sorted to the left subtree and if not it is sorted to the right one. This procedure terminates when a *leaf node* is reached. The final prediction of the ensemble $T(x)$ is obtained by combining the predicted leaf values for each tree in the ensemble. In gradient boosting, the class probability is computed by applying a sigmoid transformation to the sum of the leaf values.

2.2. Evasion Attacks

An *evasion attack* involves carefully manipulating valid inputs x into adversarial examples \tilde{x} in order to evoke a misprediction (Kantchelian et al., 2016). More formally, we use the same definition of adversarial examples as used in existing work on tree ensembles (Kantchelian et al., 2016; Chen et al., 2019a; Devos et al., 2021a) and say that \tilde{x} is an **adversarial example** for normal example x when (1) $\|\tilde{x} - x\|_\infty < \delta$ where δ is a user-selected maximum dis-

tance (i.e., the two are sufficiently close), (2) the ensemble predicts the correct label for x , and (3) the model’s predicted labels for \tilde{x} and x differ.

We now briefly describe the two existing adversarial example generation methods $\mathcal{A} : (\mathbf{T}, x, \delta, t_{\max}) \rightarrow \{SAT(\tilde{x}), UNSAT, TIMEOUT\}$ used in this paper: *kantchelian* (Kantchelian et al., 2016) and *veritas* (Devos et al., 2021a). These methods take as input an ensemble \mathbf{T} , a normal example x , a maximum perturbation size δ , and a timeout t_{\max} . They output $SAT(\tilde{x})$, where \tilde{x} is an adversarial example for x , $UNSAT$, indicating that no adversarial example exists, or $TIMEOUT$, indicating that no result could be found within timeout t_{\max} . Timeouts are explicitly handled because adversarial example generation is NP-hard (Kantchelian et al., 2016).

kantchelian formulates the adversarial example generation task as a mixed-integer linear program (MILP) and uses a generic MILP solver (e.g., Gurobi (Gurobi Optimization, LLC, 2023)). Specifically, *kantchelian* directly minimizes the $\delta = \|x - \tilde{x}\|_\infty$ value. Given an example x , it computes:

$$\min_{\tilde{x}} \|x - \tilde{x}\|_\infty \quad \text{subject to} \quad T(x) \neq T(\tilde{x}). \quad (1)$$

This approach exploits the fact that a tree ensemble can be viewed as a set of linear (in)equalities. Three sets of MILP variables are used. *Predicate variables* p_i represent the split conditions, i.e., each p_i logically corresponds to a split on an attribute f : $p_i \equiv f < \tau$. *Leaf variables* l_i indicate whether a leaf node is active. The *bound variable* b represents the l_∞ distance between the original example x and the adversarial example \tilde{x} . Constraints between the variables encode the structure of the tree. A set of predicate consistency constraints encode the ordering between splits. For example, if two split values $\tau_1 < \tau_2$ appear in the tree for attribute f , and $p_1 \equiv f < \tau_1$ and $p_2 \equiv f < \tau_2$, then $p_1 \implies p_2$. Leaf consistency constraints enforce that a leaf is only active when the splits on the root-to-leaf path to that leaf are satisfied. Lastly, the mislabel constraint requires the output to be a certain class: for leaf values v_i , $\sum_i v_i l_i \leq 0$. The objective directly minimizes the *bound variable*.

veritas improves upon *kantchelian* in terms of run time by formulating the adversarial example generation problem as a heuristic search problem in a graph representation of the ensemble (originally proposed by (Chen et al., 2019b)). The nodes in this graph correspond to the leaves in the trees of the ensemble. Guided by a heuristic, the search then repeatedly selects compatible leaves. Leaves of two different trees are compatible when the conjunction of the split conditions along the root-to-leaf paths of the leaves are logically consistent. For a given δ , *veritas* solves the

following optimization problem:¹

$$\underset{\tilde{x}}{\text{optimize}} \mathbf{T}(\tilde{x}) \quad \text{subject to} \quad \|x - \tilde{x}\|_{\infty} < \delta \quad (2)$$

The output of the model $\mathbf{T}(\tilde{x})$ is maximized when the target class for \tilde{x} is positive, and minimized otherwise. While *veritas* can also be used to directly optimize δ , in this paper we will use a predefined δ for *veritas*.

3. Method

Adversarial example generation methods like *kantchelian* and *veritas* are typically applied in the following setting:

Given a tree ensemble \mathbf{T} , a set of test examples V , and a maximum perturbation size δ ,

Generate adversarial examples for each $x \in V$.

The goal of this paper is to exploit the fact that adversarial examples are sequentially generated for each example in V . By analyzing previously found adversarial examples, we aim to improve the efficiency of adversarial example generation algorithms by biasing the search towards the perturbations that most likely to lead to an adversarial example.

Our hypothesis is that some parts of the ensemble are disproportionately sensitive to small perturbations, i.e., crossing the thresholds of split conditions in these parts of the ensemble results in large changes in the predicted value. Prior work has hypothesized that robustness is related to fragile features and that such features are included in models because learners search for any signal that improves predictive performance (Ilyas et al., 2019). One would expect that the attributes used in the split conditions in these disproportionately sensitive parts are exploited by adversarial examples more frequently than other attributes.

Figure 1 illustrates this point by showing how often each attribute is perturbed in a set of a 10 000 adversarial examples generated by *kantchelian* for two different datasets. The bar plots distinguish three categories of attributes: attributes that are never modified by any adversarial example (left), attributes that are modified by at least one but at most 5% of all adversarial examples (middle), and attributes that are modified by more than 5% of the adversarial examples. Less than 10% of the attributes are used by more than 5% of the adversarial examples. Thus the two questions are **(1) how can one identify these frequently-modified attributes and (2) how can algorithms exploit this knowledge to more quickly generate adversarial examples.**

At a high level, our proposed approach has two parts. The first part simplifies the search for adversarial examples by only allowing perturbations to a limited subset of features.

¹Note that we are abusing terminology: here, $\mathbf{T}(x)$ is the predicted probability. Previously, it was the predicted label.

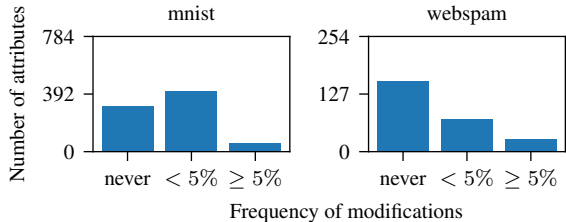


Figure 1. Bar plots showing that most attributes are not modified by the majority of adversarial examples (*mnist* and *webspam* only). The leftmost bar shows the number of attributes that are never changed by any of the 10,000 generated adversarial examples. The middle bar shows the number of attributes that are modified at least once but at most by 5% of the adversarial examples. The rightmost bar shows the number of frequently modified features.

This is accomplished by exploiting the knowledge that certain feature values are fixed, which enables simplifying the ensemble by pruning away branches that can never be reached. The second part identifies a subset of commonly perturbed features by counting how often each feature is perturbed by adversarial examples (Section 3.2). The size of this subset is determined by applying a theoretically grounded statistical test.

3.1. Modifying the Search Procedure

Our proposed approach speeds up the adversarial example generation procedure by limiting the scope of the adversarial perturbations to a subset of features F_S . This section assumes that we are given such a subset of features. The next section covers how to identify these features.

We consider three settings: *full*, *pruned*, and *mixed*. The *full* setting corresponds to the original configuration of *kantchelian* and *veritas*: the methods may perturb any attribute within a certain maximum distance δ . That is, for each attribute $f \in F$ with value x_f , the attribute values are limited to $[x_f - \delta, x_f + \delta]$. Algorithm 1 summarizes the *pruned* and *mixed* approaches. We now describe both in greater detail.

Pruned Approach The *pruned* setting disallows modifications to the attributes in the *non-selected* set of attributes $F_{NS} = F \setminus F_S$. We accomplish this by pruning the trees in the ensemble. Any node splitting on attributes in F_{NS} is removed. Its parent node is directly connected to the only child node that can be reached by examples with the fixed value for the attribute. Figure 2 shows an example of this procedure. We refer to this procedure as $\text{PRUNE}(\mathbf{T}, F_S, x)$. The adversarial example methods can be applied as normal to the pruned ensemble, but they will only generate adversarial examples with perturbations to the attributes in F_S . Pruning simplifies the MILP problem of *kantchelian* because all predicate variables p_i that correspond to

splits in internal nodes of pruned subtrees, and leaf variables l_i that correspond to leaves of pruned subtrees can be removed from the mathematical formulation. For *veritas*, the search space is reduced in size because the pruned leaves are removed from the graph representation of the ensemble. Hence, for both systems, on average, the problem difficulty is reduced by pruning the ensembles.

Pruning the trees does not affect the validity of generated adversarial examples: If \tilde{x} is an adversarial example generated for a normal example x generated on a pruned ensemble, then \tilde{x} is also an adversarial example for the full ensemble.

Proposition 3.1. *Given normal example x that is correctly classified by the full ensemble \mathbf{T}_{full} . Let $\mathbf{T}_{prun} = \text{PRUNE}(\mathbf{T}_{full}, F_S, x)$ and $\tilde{x} = \mathcal{A}(\mathbf{T}_{prun}, x, \delta, t_{max}^{prun})$ (i.e., $\mathbf{T}_{prun}(x) \neq \mathbf{T}_{prun}(\tilde{x})$ and $\|x - \tilde{x}\|_\infty < \delta$). Then it holds that $\mathbf{T}_{full}(x) \neq \mathbf{T}_{full}(\tilde{x})$.*

Proof. Because only branches not visited by x are removed, $\mathbf{T}_{prun}(x) = \mathbf{T}_{full}(x)$. The values for features in F_{NS} are fixed, so these values are equal between x and \tilde{x} . Hence, \tilde{x} only visits branches in \mathbf{T}_{full} that are also in \mathbf{T}_{prun} . Therefore, $\mathbf{T}_{prun}(\tilde{x}) = \mathbf{T}_{full}(\tilde{x})$. \square

However, an *UNSAT* generated on a pruned ensemble is inconclusive. That is, it might still be the case that an adversarial example exists for the full ensemble, albeit one with perturbations to features in F_{NS} . The *pruned* setting generates a **false negative** if it reports *UNSAT*, yet the *full* setting reports *SAT*.

Mixed Approach The *mixed* setting takes advantage of the fast adversarial generation capabilities of the *pruned* setting, but falls back to the *full* setting when the *pruned* setting returns an *UNSAT* or times out. A much stricter timeout t_{max}^{prun} is used for the *pruned* setting to fully take advantage of the fast *SATs*, while avoiding spending time on an uninformative *UNSAT*. The *mixed* setting is guaranteed to find an adversarial example if the *full* setting can find one.

Theorem 3.2. *Assume a normal example x and maximum distance δ . If an adversarial example can be found for the full ensemble \mathbf{T}_{full} , then the mixed setting is guaranteed to find an \tilde{x} such that $\|x - \tilde{x}\|_\infty < \delta$ and $\mathbf{T}_{full}(x) \neq \mathbf{T}_{full}(\tilde{x})$.*

Proof. The mixed setting first operates on the pruned ensemble \mathbf{T}_{prun} using a tight timeout and optimizes Equation 1 or 2 using *kantchelian* or *veritas* respectively. This returns (1) an adversarial example \tilde{x} , (2) an *UNSAT* or (3) times out. In case (1), the generated adversarial example \tilde{x} is also an adversarial example for the full ensemble (Prop 3.1). In cases (2) and (3), the *mixed* setting falls back to the *full* setting operating on the full ensemble \mathbf{T}_{full} with the same timeout. Hence, it inherits the full method’s guarantees. \square

Algorithm 1 Fast repeated adversarial example generation

```

1: parameters: maximum perturbation size  $\delta$ , timeouts
    $t_{max}^{full}$  and  $t_{max}^{prun}$  for full and pruned, generation method
    $\mathcal{A} : (\mathbf{T}, x, \delta, t) \rightarrow \{\text{SAT}(\tilde{x}), \text{UNSAT}, \text{TIMEOUT}\}$ 
2: function GENERATE( $\mathbf{T}_{full}, \mathcal{D}, F_S, mixed$  flag)
3:    $\tilde{\mathcal{D}} \leftarrow \emptyset$ 
4:   for  $x \in \mathcal{D}$  do
5:      $\mathbf{T}_{prun} \leftarrow \text{PRUNE}(\mathbf{T}_{full}, F_S, x)$  (Sec. 3.1)
6:      $\alpha \leftarrow \mathcal{A}(\mathbf{T}_{prun}, x, \delta, t_{max}^{prun})$ 
7:     if  $\alpha \neq \text{SAT}(\tilde{x}) \wedge mixed$  flag set then
8:        $\alpha \leftarrow \mathcal{A}(\mathbf{T}_{full}, x, \delta, t_{max}^{full})$ 
9:     end if
10:     $\tilde{\mathcal{D}} \leftarrow \tilde{\mathcal{D}} \cup \{\alpha\}$ 
11:  end for
12:  return:  $\tilde{\mathcal{D}}$ 
13: end function
    
```

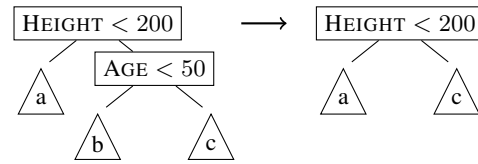


Figure 2. An example tree using two attributes HEIGHT and AGE (left). Suppose $F_{NS} = \{\text{AGE}\}$. Given an example where AGE = 55, we can prune away the internal node splitting on AGE. In the resulting tree (right), subtree (b) is pruned because it is unreachable given that AGE = 55 and only subtrees (a) and (c) remain.

3.2. Identifying Relevant Features

A good subset of relevant attributes F_S should satisfy two properties. First, it should minimize the number of false negatives, which occur when the *pruned* approach reports *UNSAT*, but the *full* approach reports *SAT*. Second, the feature subset should be small. The smaller F_S is, the more the ensemble can be pruned, and the faster the speedup is. These two objectives are somewhat in tension. Including more features will reduce the number of false negatives, but limit speeds up that are possible whereas using a very small subset will restrict the search too much resulting in many false negatives (or slow calls to the full search in the *mixed* setting). The procedure is given in Algorithm 2.

We address the first requirement by adding features to the subset that are frequently perturbed by adversarial examples. We rank features by counting how often each one differs between the perturbed adversarial examples in $\tilde{\mathcal{D}}$ so far and their corresponding normal examples in \mathcal{D} .

The second requirement is met by statistically testing whether the identified subset guarantees that the false negative rate is smaller than a given threshold with probability at least $1 - \delta$, for a specified confidence parameter δ . If it is

not guaranteed, then the subset is expanded. This is done at most 4 times for subsets of 5%, 10%, 20%, 30% of the features. If all tests fail, then a final feature subset of 40% of the most commonly modified features is used. We do not go beyond 40% because using the full feature set is then more efficient (`EXPANDFEATURESET`($F_S, \mathcal{D}, \tilde{\mathcal{D}}$) in Algorithm 2). Each test is executed on a small set of n generated adversarial examples. A first zeroth set is used merely for obtaining the first feature counts.

Next we give the details of how these tests are performed. Take $\mathcal{D}_F = (x_1, x_2, \dots, x_N)$ the dataset we use to find the feature subset F_S . We define $\mathbf{v} = (v_1, v_2, \dots, v_N)$ to be the binary vector such that $v_i = 1$ if the *pruned* search with the feature subset F_S returns *UNSAT* for the example x_i but the *full* search returns *SAT*, and $v_i = 0$ otherwise. Then the true false negative rate corresponding to F_S can be written as $FNR = \frac{1}{N} \sum_{i=1}^N v_i$. Now, the small set of n examples from which we are estimating the false negative rate is a random vector $\mathbf{X} = (X_1, X_2, \dots, X_n)$ sampled without replacement from \mathcal{D}_F . We also define $\mathbf{V} = (V_1, V_2, \dots, V_n)$ where V_i is the random variable defined analogously to how we defined v_i . It follows that $\sum_{i=1}^n V_i$ is distributed as a hypergeometric random variable. Our null hypothesis is that FNR is greater than the threshold τ . We reject the hypothesis if $\bar{V} = \frac{1}{n} \sum_{i=1}^n V_i$ takes a value smaller than the threshold by more than a margin Δ . Next we bound the probability that, this happens, i.e., the probability $P[\bar{V} \leq \tau - \Delta]$, under the null hypothesis $FNR \geq \tau$:

$$\begin{aligned} P[\bar{V} \leq \tau - \Delta] &= P[\bar{V} - FNR \leq \tau - \Delta - FNR] \\ &\leq P[\bar{V} - FNR \leq -\Delta], \end{aligned} \quad (3)$$

where the second inequality follows from the null hypothesis. Due to how we defined \bar{V} , we have $\mathbb{E}[\bar{V}] = FNR$. Moreover, $n \cdot \bar{V}$ is distributed as a hypergeometric random variable, therefore we can use an exponential bound from Greene & Wellner (2017), stated below in Theorem 3.3, to bound the probability. Since the existing theorem bounds $P[\bar{X}_n - \mu \geq \varepsilon]$ instead of our $P[\bar{X}_n - \mu \leq -\varepsilon]$, we provide the needed manipulations after the theorem.

Theorem 3.3 (Greene & Wellner (2017)). *Let $\bar{v} \sim \text{Hypergeometric}(n, D, N)$, a margin Δ as in Equation 3, and $\lambda = \Delta\sqrt{n}$. Suppose $N > 4$ and $2 \leq n < D \leq N/2$. Then, for all $0 < \Delta < 1/2$:*

$$\begin{aligned} P[\sqrt{n}(\bar{v} - \mu) \geq \lambda] &\leq \sqrt{\frac{1}{2\pi\lambda^2}} \left(\frac{1}{2}\right) \\ &\cdot \sqrt{\left(\frac{N-n}{N}\right) \left(\frac{\sqrt{n}+2\lambda}{\sqrt{n}-2\lambda}\right) \left(\frac{N-n+2\sqrt{n}\lambda}{N-n-2\sqrt{n}\lambda}\right)} \\ &\cdot \exp\left(-\frac{2}{1-\frac{n}{N}}\lambda^2\right) \exp\left(-\frac{1}{3}\left(1+\frac{n^3}{(N-n^3)}\right)\frac{\lambda^4}{n}\right). \end{aligned}$$

We define $W_i = 1 - V_i$, $\mu_W = 1 - FNR$ and $\Delta = \lambda/\sqrt{n}$. It is clear that if $n \cdot \bar{V}$ is hypergeometric, so is $n \cdot \bar{W} =$

$\sum_{i=1}^n W_i$.² Then we can write:

$$\begin{aligned} P[\sqrt{n}(\bar{W} - \mu_w) \geq \lambda] &= P\left[\bar{W} - \mu_w \geq \frac{\lambda}{\sqrt{n}}\right] \\ &= P\left[\frac{1}{n} \sum_{i=1}^n (1 - V_i) - 1 + FNR \geq \frac{\lambda}{\sqrt{n}}\right] \\ &= P\left[-\frac{1}{n} \sum_{i=1}^n V_i + FNR \geq \frac{\lambda}{\sqrt{n}}\right] \\ &= P[\bar{V} - FNR \leq -\Delta]. \end{aligned}$$

Here, the last expression is what we need to bound and the first is what Theorem 3.3 bounds.

In the algorithm, we are given a confidence parameter η and we determine Δ using the bound in Theorem 3.3 so that the probability of incorrectly selecting a too small subset F_S is smaller than η . Because we execute the test 4 times, we apply a union-bound correction of factor 4. Choosing a confidence of 90%, we extract $\Delta \in \{1/n, 2/n, \dots, 1/2\}$ by computing the bound and stopping at the smallest Δ such that $P[\bar{V} \leq \tau - \Delta] < \eta/4$. Note that there is a trade-off. The higher n , the better the statistical estimates and the counts are, but also the more examples we process with a potentially suboptimal feature subset.

Algorithm 2 Find feature subset

- 1: $F_S \leftarrow \emptyset$
 - 2: **for** $k \in 0..4$ **do**
 - 3: $\tilde{\mathcal{D}} \leftarrow \text{GENERATE}(\mathbf{T}, \mathcal{D}[kn, k(n+1)], F_S, \text{true})$
 - 4: $\bar{v} \leftarrow \frac{1}{n} \times$ number of false negatives in $\tilde{\mathcal{D}}$
 - 5: **if** \bar{v} exceeds $\tau - \Delta$, **then** F_S , selecting most frequently perturbed features in $\tilde{\mathcal{D}}$ first.
 - 6: **else break** the loop
 - 7: **end for**
-

4. Experiments

Empirically, we address the following questions:

- Q1 Is our approach able to improve the run time performance of generating adversarial examples?
- Q2 How does ensemble complexity affect our approach's performance?
- Q3 What is our empirical false negative rate?

Because the described procedure is based on identifying a subset of relevant features, it makes sense to exploit it only

²Moreover, for any reasonably small acceptable FNR threshold τ , with high probability we will either get $\bar{V} > \tau$ or it will hold $n < D$ where D is the parameter of the hypergeometric distribution for $n \cdot \bar{W}$, allowing us to use the bound from Theorem 3.3.

when the dataset has a large number of dimensions. Therefore, we present numerical experiments for ten classification tasks on high-dimensional datasets, using both tabular data and image data, as shown in Table 1.

Table 1. Datasets’ characteristics: N and $\#F$ are the number of examples and the number of features. We also report the adopted values of max allowed perturbation δ , for XGBoost and Random forest. *higgs* and *prostate* are random subsets of the original, bigger datasets. Multi-class classification datasets were converted to binary classification: for *covtype* we predict majority-vs-rest, for *mnist* and *fmnist*, we predict classes 0-4 vs. classes 5-9, and for *sensorless* classes 0-5 vs. classes 6-10.

Dataset	N	#F	δ XGB	δ RF
covtype	581k	54	0.1	0.3
fmnist	70k	784	0.3	0.3
higgs	250k	33	0.08	0.08
miniboone	130k	51	0.08	0.08
mnist	70k	784	0.3	0.3
prostate	100k	103	0.1	0.2
roadsafety	111k	33	0.06	0.12
sensorless	58.5k	48	0.06	0.12
vehicle	98k	101	0.15	0.15
webspam	350k	254	0.04	0.06

4.1. Experimental Setup

We apply 5-fold cross validation for each dataset. We use four of the folds to train an XGBoost or a random forest ensemble T . From the test set, we randomly sample 10 000 normal examples and attempt to generate adversarial examples by perturbing each one using the *veritas* or *kantchelian* attack. Each ensemble’s hyperparameters are tuned using the grid search described in Appendix B. The experiments ran on an Intel(R) E3-1225 CPU with 32GiB of memory.

The *pruned* and *mixed* settings work as follows. We use the procedure from Section 3.2 to select a subset of relevant features. Using Theorem 3.3, we find $n = 100$ and $\Delta = 0.1$. This gives us a $1 - \eta = 90\%$ confidence that our true false negative rate is below $\tau = 25\%$. We then apply Algorithm 2: we generate 5 sets of n adversarial examples to (1) find which features are perturbed most often and (2) determine the size of the feature subset F_S . After Algorithm 2 terminates, F_S is fixed, and we run the *pruned* and *mixed* settings on all the remaining test examples (Algorithm 1).

We set a timeout of one minute for the *full* setting, and a much stricter timeout of 1 (*kantchelian*) or 0.1 (*veritas*) seconds in the *pruned* setting. We can be stricter with *veritas* as it is an approximate method that is faster than the exact *kantchelian*.

4.2. Q1: Run time

Table 2 reports the average run time for the *full* setting and the average speedup given by the *pruned* and *mixed* settings. Our approach consistently speeds up *kantchelian* with the *pruned* approach yielding speedups between 2.4x-25.4x, and *mixed* between 1.6x-7.1x. Using *veritas*, we achieve speedups of between 1.6x-35.9x with the *pruned* approach, and between 1.0x-4.5x with the *mixed* approach.

Generally, *kantchelian* benefits slightly more than *veritas* regardless of which setting is used. This is because *veritas* is already an approximate approach and its existing heuristics leave less room for improvement. In contrast, the feature pruning can greatly simplify the MILP problem, which consequently leads to faster run times.

The story is more complicated when considering the ensemble type. On XGB ensembles, both settings offer consistent wins. The *mixed* setting falls back to the *full* search on average 8% of the time, regardless of the attack.³ This helps it achieve a speedup by taking advantage of the fast *SAT* results of the *pruned* setting while still offering the theoretical guarantee from Theorem 3.2.

However, generating adversarial examples is more difficult for random forests (RF) than XGB.⁴ This leads to the *pruned* strategy offering larger wins than for XGB ensembles. For the RF ensembles, the *pruned* setting often hits its timeout limit or fails more often, which leads to calls to the *full* search 22% of the time.

Figure 3 shows the number of executed searches as a function of time in the four combinations of attack type and model type, for a selected four datasets.⁵ For XGB, both attacks benefit. Moreover, the *mixed* setting is typically very close in run time to the *pruned*. On RF, we see that the *pruned* setting offers larger speedups. However, we see a more noticeable difference between it and the *mixed* search on several datasets. This indicates that the *mixed* strategy most fall back more often to an expensive *full* search.

Finally, it is natural to wonder how the quality of the generated adversarial examples is affected by the modified search procedure. While this is difficult to quantify, Figure 4 provides some examples of constructed adversarial examples for the *mnist* dataset. Visually, the examples constructed by *full* and *pruned* for both attacks are very similar. The examples constructed using *kantchelian* look more similar to the base example than those for *veritas* because *kantchelian* finds the closest possible adversarial example whereas *veritas* has a different objective: it constructs an adversarial

³See Table 5 in the supplement

⁴When running *kantchelian* the *full* search hit the global time out of 6 hours, meaning that it terminated before attempting to generate 10,000 adversarial examples on six of the datasets.

⁵The supplement shows these plots for all datasets.

Table 2. Average run times and speedups to verify 10 000 test examples using *kantchelian/veritas* on an XGBoost/random forest ensemble for all three approaches: *full*, *pruned* and *mixed*. A star denotes that the dataset exceeded the six hour global timeout.

	Kantchelian XGB			Kantchelian RF			Veritas XGB			Veritas RF		
	<i>full</i>	<i>pruned</i>	<i>mixed</i>	<i>full</i>	<i>pruned</i>	<i>mixed</i>	<i>full</i>	<i>pruned</i>	<i>mixed</i>	<i>full</i>	<i>pruned</i>	<i>mixed</i>
covtype	7.7m	3.0×	2.3×	5.6h	25.4×	6.6×	6.4s	1.6×	1.4×	1.1m	7.0×	1.6×
fmnist	1.3h	6.6×	4.7×	4.8h	7.6×	7.1×	1.2m	1.6×	1.5×	6.9m	3.6×	3.1×
higgs	3.7h	2.8×	1.6×	6.0h*	3.3×	1.0×	1.4m	7.5×	1.5×	59.8m	13.7×	2.4×
miniboone	2.7h	5.1×	3.6×	6.0h*	4.5×	1.1×	3.7m	15.3×	1.7×	3.0h	19.2×	2.0×
mnist	20.0m	6.3×	5.5×	2.7h	9.8×	5.8×	1.1m	2.3×	1.9×	3.7m	2.9×	2.7×
prostate	11.8m	3.5×	3.0×	6.0h*	2.7×	1.3×	12.4s	2.3×	2.1×	23.0m	25.2×	2.6×
roadsafety	10.3m	2.4×	2.0×	5.8h	10.2×	2.4×	10.4s	2.1×	1.7×	52.2m	35.9×	4.5×
sensorless	27.1m	2.8×	2.4×	6.0h*	5.4×	2.9×	12.9s	2.2×	1.8×	3.0m	5.4×	1.8×
vehicle	2.4h	4.4×	3.1×	6.0h*	3.8×	1.4×	12.0m	19.9×	3.8×	43.6m	5.8×	1.0×
webspam	23.7m	5.6×	4.3×	6.0h*	12.2×	7.2×	25.8s	2.4×	2.0×	12.5m	3.6×	1.1×

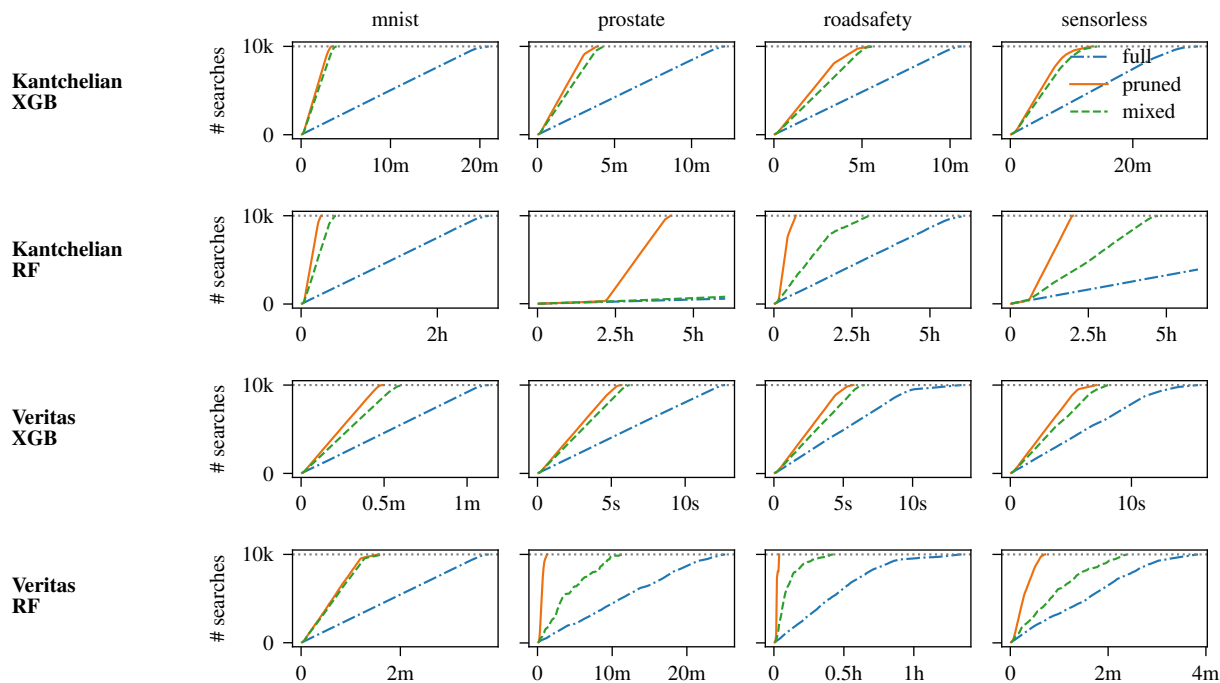


Figure 3. Average run times for 10 000 calls to *full*, *pruned* and *mixed* for *kantchelian* (top) and *veritas* (bottom). Results are given for both XGBoost and random forest for four selected datasets.

example that will explicit a highly confident misprediction. See Appendix D for more generated examples.

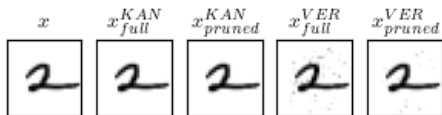


Figure 4. Generated adversarial examples for base example x from *mnist*, with both attacks and both *full* and *pruned* setting.

4.3. Q2: Scaling Behavior

Two key hyperparameters of XGB and RF are the maximum depth of each learned tree and the number of trees in the ensemble. We explore how varying these affects the considered approach employing the same setup as described in Subsection 4.1. We use the *mnist* dataset and omit *kantchelian* with RFs due to its computational cost.

Figure 5 (top) shows how the run time to perform 10,000 searches varies as function of the maximum tree depth for a fixed ensemble size of 50 for XGB and 25 for RF. The run times for the *pruned* and *mixed* approaches grow very

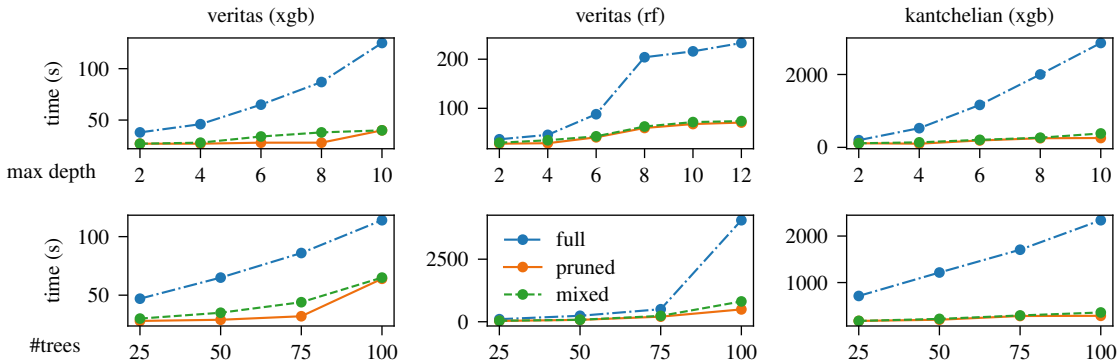


Figure 5. Run time of *full*, *mixed* and *pruned* settings for varying the max depth (top) and number of estimators in the ensemble (bottom).

slowly as the depths are increased. In contrast, the *full* search scales worse: deeper trees lead to higher run times.

Figure 5 (bottom) shows how the run time to perform 10,000 searches varies as function of the ensemble size for a fixed maximum tree depth of 6 for XGB and 10 for RF. Again, the *pruned* and *mixed* approaches show much better scaling behavior. Note that *veritas*’s full search shows a very large jump on RF when moving from 75 to 100 trees. These results indicate that our approaches will offer even better run time performance than the standard full search for more complex ensembles.

4.4. Q3: Empirical FNR

We use Equation 3 to bound the false negative rate to be less than 25% with high probability. Table 5 in the supplement reports the empirical false negative rates for all experiments. The average false negative rate is 6.4% and the maximum is 11.8%. Hence, empirically we achieve better results than the theory guarantees. Neither the ensemble method nor the attack type strongly influence the false negative rate.

Still, we observe that with these false negative rates we can dramatically reduce the number of considered features. On average, F_S contains 19.1% of the features. Out of 200 experiments,⁶ we only select the maximum percentage of features 15 times. Generally, *kantchelian* requires slightly more features than *veritas* and RF models requires slightly more features than XGB models.

5. Related Work

Adversarial examples have been theoretically studied and defined in multiple different ways (Diochnos et al., 2018; Gourdeau et al., 2021). Approaches to reason about learned tree ensembles have received substantial interest in recent

years. These include algorithms for performing evasion attacks (Kantchelian et al., 2016; Einziger et al., 2019) (i.e., generate adversarial examples), perform robustness checking (Chen et al., 2019b), and verify that the ensembles satisfy certain criteria (Devos et al., 2021b;a; Ranzato & Zanella, 2020; Törnblom & Nadjm-Tehrani, 2020). Kantchelian et al. (2016) were the first to show that, just like neural networks, tree ensembles are susceptible to evasion attacks. Their MILP formulation is still the most frequently used method to check robustness and generate adversarial examples. Beyond this exact approach, several approximate approaches exist (Chen et al., 2019b; Devos et al., 2021a; Wang et al., 2020; Zhang et al., 2020) though not all of them are able to generate concrete adversarial examples (e.g., (Chen et al., 2019b; Wang et al., 2020)).

Other work focuses on making tree ensembles more robust. Approaches for this include adding generated adversarial examples to the training data (model hardening) (Kantchelian et al., 2016), or modifying the splitting procedure (Chen et al., 2019a; Calzavara et al., 2020; Vos & Verwer, 2021). Gaining further insights into how evasion attacks target tree ensembles, like those contained in this paper, may inspire novel ways to improve the robustness of learners.

6. Conclusions

This paper explored two methods to efficiently generate adversarial examples for tree ensembles. We showed that considering only the *same subset of features* is typically sufficient to generate adversarial examples for tree ensemble models. We proposed a simple procedure to quickly identify such a subset of features, and two generic approaches that exploit it to speed up adversarial examples generation. We showed how to apply them to an exact (*kantchelian*) and approximate (*veritas*) evasion attack on tree ensembles, and discussed their properties and run time performances.

⁶5 folds x 10 datasets x 2 ensemble x 2 attacks

Acknowledgments

This research is supported by The European Union’s Horizon Europe Research and Innovation program under the grant agreement TUPLES No. 101070149 (LC, LD, OK, JD), the Research Foundation-Flanders (FWO, LD: 1SB1322N), and the Flemish Government under the “Onderzoeksprogramma Artificiële Intelligentie (AI) Vlaanderen” program (JD).

Broader Impact Statement

Machine learning is widely used in many different application areas. With the wide adoption, machine learned models, including tree ensembles, increasingly become high-stake targets for attackers who might employ evasion attacks to achieve their goal.

While this work proposes ways to speed up attacks, we feel it is important to shed light on things that adversaries may do. Moreover, insights about possible attacks increase our understanding and may hence yield insights that result in improved defenses or ways to make tree ensembles more robust.

We strongly feel that it is in the interest of the research community that (1) the research community stays on top of these developments so that machine learning libraries can adapt if necessary, and (2) all work done in this area is open-access. For that reason, source codes used in this work will be made available upon acceptance.

References

- Andriushchenko, M. and Hein, M. Provably robust boosted decision stumps and trees against adversarial attacks. In *Advances in Neural Information Processing Systems*, volume 32, 2019.
- Breiman, L. Random forests. *Machine learning*, 45:5–32, 2001.
- Calzavara, S., Lucchese, C., Tolomei, G., Abebe, S. A., and Orlando, S. Treant: training evasion-aware decision trees. *Data Mining and Knowledge Discovery*, 34(5): 1390–1420, 2020.
- Chen, H., Zhang, H., Boning, D., and Hsieh, C.-J. Robust decision trees against adversarial examples. In *International Conference on Machine Learning*, pp. 1122–1131, 2019a.
- Chen, H., Zhang, H., Si, S., Li, Y., Boning, D., and Hsieh, C.-J. Robustness verification of tree-based models. *Advances in Neural Information Processing Systems*, 32, 2019b.
- Chen, T. and Guestrin, C. XGBoost: A scalable tree boosting system. In *Proceedings of the 22nd ACM SIGKDD International Conference on Knowledge Discovery and Data Mining*, pp. 785–794, 2016.
- Devos, L., Meert, W., and Davis, J. Versatile verification of tree ensembles. In *Proceedings of the 38th International Conference on Machine Learning*, volume 139 of *Proceedings of Machine Learning Research*, pp. 2654–2664, 2021a.
- Devos, L., Meert, W., and Davis, J. Verifying tree ensembles by reasoning about potential instances. In *Proceedings of the 2021 SIAM International Conference on Data Mining (SDM)*, pp. 450–458. SIAM, 2021b. doi: 10.1137/1.9781611976700.51. URL <https://epubs.siam.org/doi/abs/10.1137/1.9781611976700.51>.
- Devos, L., Cascioli, L., and Davis, J. Robustness verification of multiclass tree ensembles. *Proceedings of the AAAI Conference on Artificial Intelligence*, 38:To appear, 2024.
- Diochnos, D. I., Mahloujifar, S., and Mahmoody, M. Adversarial risk and robustness: General definitions and implications for the uniform distribution. In *Neural Information Processing Systems*, 2018. URL <https://api.semanticscholar.org/CorpusID:53097516>.
- Einzig, G., Goldstein, M., Sa’ar, Y., and Segall, I. Verifying robustness of gradient boosted models. *Proceedings of the AAAI Conference on Artificial Intelligence*, 33:2446–2453, 2019. doi: 10.1609/aaai.v33i01.33012446. URL <https://ojs.aaai.org/index.php/AAAI/article/view/4089>.
- Friedman, J. H. Greedy function approximation: a gradient boosting machine. *Annals of statistics*, pp. 1189–1232, 2001.
- Goodfellow, I. J., Shlens, J., and Szegedy, C. Explaining and harnessing adversarial examples. *arXiv preprint arXiv:1412.6572*, 2014.
- Gourdeau, P., Kanade, V., Kwiatkowska, M., and Worell, J. On the hardness of robust classification. *Journal of Machine Learning Research*, 22(273):1–29, 2021. URL <http://jmlr.org/papers/v22/20-285.html>.
- Greene, E. and Wellner, J. A. Exponential bounds for the hypergeometric distribution. *Bernoulli: official journal of the Bernoulli Society for Mathematical Statistics and Probability*, 23(3):1911, 2017.
- Guo, J.-Q., Teng, M.-Z., Gao, W., and Zhou, Z.-H. Fast provably robust decision trees and boosting. In *Proceedings of the 39th International Conference on Machine Learning*

- Learning*, volume 162 of *Proceedings of Machine Learning Research*, pp. 8127–8144, 2022.
- Gurobi Optimization, LLC. Gurobi Optimizer Reference Manual, 2023. URL <https://www.gurobi.com>.
- Ilyas, A., Santurkar, S., Tsipras, D., Engstrom, L., Tran, B., and Madry, A. Adversarial examples are not bugs, they are features. In Wallach, H., Larochelle, H., Beygelzimer, A., d’Alché-Buc, F., Fox, E., and Garnett, R. (eds.), *Advances in Neural Information Processing Systems*, volume 32. Curran Associates, Inc., 2019. URL https://proceedings.neurips.cc/paper_files/paper/2019/file/e2c420d928d4bf8ce0ff2ec19b371514-Paper.pdf.
- Kantchelian, A., Tygar, J. D., and Joseph, A. Evasion and hardening of tree ensemble classifiers. In *International Conference on Machine Learning*, pp. 2387–2396, 2016.
- Pedregosa, F., Varoquaux, G., Gramfort, A., Michel, V., Thirion, B., Grisel, O., Blondel, M., Prettenhofer, P., Weiss, R., Dubourg, V., Vanderplas, J., Passos, A., Cournapeau, D., Brucher, M., Perrot, M., and Duchesnay, E. Scikit-learn: Machine learning in Python. *Journal of Machine Learning Research*, 12:2825–2830, 2011.
- Ranzato, F. and Zanella, M. Abstract interpretation of decision tree ensemble classifiers. In *Proceedings of the AAAI Conference on Artificial Intelligence*, volume 34, pp. 5478–5486, 2020.
- Szegedy, C., Zaremba, W., Sutskever, I., Bruna, J., Erhan, D., Goodfellow, I., and Fergus, R. Intriguing properties of neural networks. *arXiv preprint arXiv:1312.6199*, 2013.
- Törnblom, J. and Nadjm-Tehrani, S. Formal verification of input-output mappings of tree ensembles. *Science of Computer Programming*, 194:102450, 2020.
- Vos, D. and Verwer, S. Efficient training of robust decision trees against adversarial examples. In *Proceedings of the 38th International Conference on Machine Learning*, volume 139 of *Proceedings of Machine Learning Research*, pp. 10586–10595, 2021.
- Vos, D. and Verwer, S. Robust optimal classification trees against adversarial examples. In *Proceedings of the AAAI Conference on Artificial Intelligence*, volume 36, pp. 8520–8528, 2022a.
- Vos, D. and Verwer, S. Adversarially robust decision tree relabeling. In *Joint European Conference on Machine Learning and Knowledge Discovery in Databases*, 2022b.
- Wang, Y., Zhang, H., Chen, H., Boning, D., and Hsieh, C.-J. On l_p -norm robustness of ensemble decision stumps and trees. In *Proceedings of the 37th International Conference on Machine Learning*, volume 119 of *Proceedings of Machine Learning Research*, pp. 10104–10114. PMLR, 13–18 Jul 2020. URL <https://proceedings.mlr.press/v119/wang20aa.html>.
- Zhang, C., Zhang, H., and Hsieh, C.-J. An efficient adversarial attack for tree ensembles. In *Advances in Neural Information Processing Systems*, volume 33, pp. 16165–16176, 2020.

A. Analysis of the Problem Setting

Adversarial examples are generated for tasks like computing adversarial accuracy, computing empirical robustness, and performing model hardening. The effect of using the approximation proposed in this paper differs for each task.

Computing the adversarial accuracy of a classifier only requires determining whether an adversarial example \tilde{x} exists within the given δ for each provided normal example x . Because the *mixed* strategy reverts to the original complete search when the *pruned* approach returns an *UNSAT*, as stated in Theorem 3.2 it is guaranteed to find an adversarial example if it exists. Hence, the *mixed* strategy can speed up computing the adversarial accuracy without affecting its value.

Computing the empirical robustness of a classifier requires finding the nearest adversarial example \tilde{x} for each normal example x . Because the *pruned* approach does not consider all features and the *mixed* approach may not, they may return an adversarial example that is further away than if the full search space was considered. Hence, when using an exact attack like *kantchelian*, the empirical robustness computed using the *mixed* strategy is an overestimate of the true empirical robustness. We show this and we study what happens with an approximate method in Appendix D.

In model hardening, a large number of adversarial examples are generated and added to the training data (Kantchelian et al., 2016). The *pruned* approach can be used to generate a lot more adversarial examples in a fixed amount of time.

B. Employed Datasets and Models

Table 3 gives specific reference to each of the datasets used in the experiments.

We tune ensemble-specific hyperparameters through grid search. In both model types, we choose the number of trees in $\{10, 20, 50\}$. Max depth is chosen in the range $[3, 6]$ for XGBoost, and in $\{5, 7, 10\}$ for random forest (which typically needs deeper trees to work better). XGBoost learning rate is chosen among $\{0.1, 0.5, 0.9\}$. Table 4 reports the tuned hyperparameters of the learned ensembles after the

Table 3. References to all seven datasets used in the experiments. Selected datasets all have more than 50k examples and more than 30 features, so that adversarial example generation is typically time consuming and our methods can speed it up. Multiclass classification datasets are reduced to binary classification (classes 0-4 vs. class 5-9 for *mnist* and *fmnist*, classes 0-5 vs. classes 6-10 for *sensorless*).

Dataset	link
covtype	https://www.openml.org/d/1596
fmnist	https://www.openml.org/d/40996
higgs	https://www.openml.org/d/42769
mini-boone	https://www.openml.org/d/44128
mnist	https://www.openml.org/d/554
prostate	https://www.openml.org/d/45672
roadsafety	https://www.openml.org/d/45038
sensorless	https://archive.ics.uci.edu/dataset/325
vehicle	https://www.openml.org/d/357
webspam	https://www.csie.ntu.edu.tw/~cjlin/libsvmtools/datasets/binary.html#webspam

grid search. When running *kantchelian* on random forests, due to long run times, we had to limit the number of estimators to 25.

While the model sizes are smaller, these ensembles are already challenging for the full settings of *kantchelian* and *veritas*. This is also highlighted in Section 4.3 where we empirically study the effect of increasing the ensemble size on performance. Those results show that the *full* procedures becomes increasingly slower as the ensemble complexity grows, and our method offers larger wins.

Table 4. Learners’ tuned hyperparameters after the grid search described in Section 4. Each ensemble T has maximum tree depth d and contains M trees. The learning rate for XGBoost is η .

Dataset	XGBoost			RF	
	M	d	η	M	d
covtype	50	6	0.9	50	10
fmnist	50	6	0.1	50	10
higgs	50	6	0.1	50	10
mini-boone	50	6	0.1	50	10
mnist	50	6	0.5	50	10
prostate	50	4	0.5	50	10
roadsafety	50	6	0.5	50	10
sensorless	50	6	0.5	50	10
vehicle	50	6	0.1	50	10
webspam	50	5	0.5	50	10

C. Expanded Experimental Results

C.1. Run time

Figure 7 shows the number of executed searches as a function of time when using *veritas* attack on an XGBoost ensemble (top) or a random forest (bottom).

Table 5 shows average time to run 10,000 searches and speedups per dataset. The averages are computed over five folds. There is one table for each combination of attack (*kantchelian*, *veritas*) and ensemble type (XGB, RF). For

each dataset, we also report the average size of the relevant feature subset F_S , the percent of searches in the *mixed* setting that require making a call to the *full* search, the false negative rate (proportion of times that *pruned* returns UNSAT but *full* returns SAT), and percent of examples that were skipped due to a method reaching the global timeout of six hours.

Table 6 extends run time results of the presented experiments by also reporting standard deviations.

Finally, Figures 6 and 7 show the number of executed searches as a function of time for *kantchelian* and *veritas* on all ten datasets. Each plot contains the results for XGB (top two rows) and RF (bottom two rows). Hence these plots show the complete set of results from Figure 3 in the main paper.

C.2. Timeouts

Table 7 completes the discussion by showing the percentage of searches that timed out for each dataset, ensemble type and method. In short, XGBoost ensembles are on average easier to verify, and the searches almost never time out. On the other hand, random forests are more challenging. It can happen that with a strict timeout, the *pruned* setting is not able to find a solution, as the task remains complex even working with a reduced feature set. In those cases, *pruned* ends with a TIMEOUT and *mixed* will have to execute the full search. In particular for *kantchelian* on random forest, datasets with a lot of *pruned* timeouts are those that then hit the six hours global timeout. This is coherent with the discussion from Section 4.2.

D. Quality of Generated Adversarial Examples

We extend Figure 4 by further discussing the quality of generated adversarial examples providing more examples, and looking in detail at their distance with respect to the related base example.

Faster Repeated Evasion Attacks in Tree Ensembles

Table 5. Average run times (and speedups) to verify 10000 test examples using *kantchelian/veritas* on an XGBoost/Random forest ensemble for all three approaches: *full*, *pruned* and *mixed*. For each dataset, we also report the average size of the relevant feature subset, the number of calls to the *full* setting during *mixed* (= number of UNSAT + number of UNK for *pruned*), the number of false negatives (*pruned* returns UNSAT, but *full* returns SAT), and the percent of examples that were skipped due to a method reaching the global timeout of six hours. Experiments that exceeded such timeout are starred.

Kantchelian, XGBoost											
	<i>full</i>	<i>pruned</i>	<i>mixed</i>		% rel. feats	#full calls	#false neg.	<i>full skip</i>	<i>prune skip</i>	<i>mixed skip</i>	
covtype	7.7m	2.6m	3.0×	3.4m	2.3×	5.6%	7.5%	7.2%	0 %	0 %	0 %
fmnist	1.3h	11.3m	6.6×	15.9m	4.7×	12.3%	6.6%	6.6%	0 %	0 %	0 %
higgs	3.7h	1.3h	2.8×	2.3h	1.6×	21.2%	15.5%	1.9%	0 %	0 %	0 %
miniboone	2.7h	31.4m	5.1×	44.9m	3.6×	24.0%	11.2%	10.1%	0 %	0 %	0 %
mnist	20.0m	3.2m	6.3×	3.6m	5.5×	10.6%	2.1%	2.1%	0 %	0 %	0 %
prostate	11.8m	3.4m	3.5×	4.0m	3.0×	11.6%	7.8%	7.0%	0 %	0 %	0 %
roadsafety	10.3m	4.4m	2.4×	5.2m	2.0×	33.8%	6.2%	6.1%	0 %	0 %	0 %
sensorless	27.1m	9.7m	2.8×	11.1m	2.4×	31.7%	9.5%	9.0%	0 %	0 %	0 %
vehicle	2.4h	33.6m	4.4×	46.8m	3.1×	32.6%	10.0%	9.4%	0 %	0 %	0 %
webspam	23.7m	4.3m	5.6×	5.5m	4.3×	8.3%	5.5%	5.5%	0 %	0 %	0 %
Kantchelian, RF											
	<i>full</i>	<i>pruned</i>	<i>mixed</i>		% rel. feats	#full calls	#false neg.	<i>full skip</i>	<i>prune skip</i>	<i>mixed skip</i>	
covtype	5.6h	13.1m	25.4×	50.6m	6.6×	5.6%	11.4%	10.7%	0 %	0 %	0 %
fmnist	4.8h	37.7m	7.6×	40.3m	7.1×	20.3%	<1 %	<1 %	0 %	0 %	0 %
higgs	6.0h*	4.4h	3.3×	6.0h	1.0×	25.8%	81.5%	1.4%	83.4%	0 %	82.7%
miniboone	6.0h*	3.3h	4.5×	6.0h	1.1×	34.0%	73.7%	2.2%	78.5%	0 %	75.8%
mnist	2.7h	16.2m	9.8×	27.4m	5.8×	11.1%	8.7%	8.7%	0 %	0 %	0 %
prostate	6.0h*	4.2h	2.7×	6.0h	1.3×	10.8%	54.9%	<1 %	94.3%	0 %	92.1%
roadsafety	5.8h	34.3m	10.2×	2.4h	2.4×	26.6%	13.9%	10.6%	<1 %	0 %	0 %
sensorless	6.0h*	2.0h	5.4×	4.6h	2.9×	37.5%	15.3%	2.2%	61.1%	0 %	0 %
vehicle	6.0h*	3.4h	3.8×	6.0h	1.4×	41.0%	54.2%	1.9%	82.7%	0 %	75.8%
webspam	6.0h*	1.0h	12.2×	2.1h	7.2×	10.4%	6.3%	1.8%	67.2%	0 %	0 %
Veritas, XGBoost											
	<i>full</i>	<i>pruned</i>	<i>mixed</i>		% rel. feats	#full calls	#false neg.	<i>full skip</i>	<i>prune skip</i>	<i>mixed skip</i>	
covtype	6.4s	4.1s	1.6×	4.4s	1.4×	7.0%	5.4%	5.2%	0 %	0 %	0 %
fmnist	1.2m	46.3s	1.6×	47.2s	1.5×	10.3%	1.6%	1.4%	0 %	0 %	0 %
higgs	1.4m	11.6s	7.5×	58.0s	1.5×	21.8%	4.5%	4.1%	0 %	0 %	0 %
miniboone	3.7m	14.7s	15.3×	2.2m	1.7×	22.0%	9.4%	8.4%	0 %	0 %	0 %
mnist	1.1m	28.2s	2.3×	34.5s	1.9×	5.2%	10.6%	10.6%	0 %	0 %	0 %
prostate	12.4s	5.3s	2.3×	6.0s	2.1×	11.2%	7.9%	7.0%	0 %	0 %	0 %
roadsafety	10.4s	5.0s	2.1×	6.2s	1.7×	33.8%	9.9%	9.8%	0 %	0 %	0 %
sensorless	12.9s	5.8s	2.2×	7.2s	1.8×	21.2%	9.8%	9.3%	0 %	0 %	0 %
vehicle	12.0m	36.2s	19.9×	3.2m	3.8×	20.2%	12.2%	11.8%	0 %	0 %	0 %
webspam	25.8s	10.6s	2.4×	12.8s	2.0×	5.4%	10.1%	10.1%	0 %	0 %	0 %
Veritas, RF											
	<i>full</i>	<i>pruned</i>	<i>mixed</i>		% rel. feats	#full calls	#false neg.	<i>full skip</i>	<i>prune skip</i>	<i>mixed skip</i>	
covtype	1.1m	9.6s	7.0×	42.6s	1.6×	5.6%	11.2%	10.4%	0 %	0 %	0 %
fmnist	6.9m	1.9m	3.6×	2.2m	3.1×	10.9%	9.3%	5.0%	0 %	0 %	0 %
higgs	59.8m	4.4m	13.7×	25.1m	2.4×	33.9%	13.7%	7.4%	0 %	0 %	0 %
miniboone	3.0h	9.3m	19.2×	1.5h	2.0×	30.8%	14.8%	10.8%	0 %	0 %	0 %
mnist	3.7m	1.3m	2.9×	1.4m	2.7×	10.7%	4.9%	3.4%	0 %	0 %	0 %
prostate	23.0m	54.8s	25.2×	8.7m	2.6×	11.8%	11.0%	10.0%	0 %	0 %	0 %
roadsafety	52.2m	1.5m	35.9×	11.5m	4.5×	25.0%	8.7%	8.1%	0 %	0 %	0 %
sensorless	3.0m	32.9s	5.4×	1.7m	1.8×	21.2%	10.1%	9.7%	0 %	0 %	0 %
vehicle	43.6m	7.5m	5.8×	42.1m	1.0×	32.6%	33.6%	6.6%	0 %	0 %	0 %
webspam	12.5m	3.5m	3.6×	11.0m	1.1×	10.5%	12.7%	2.0%	0 %	0 %	0 %

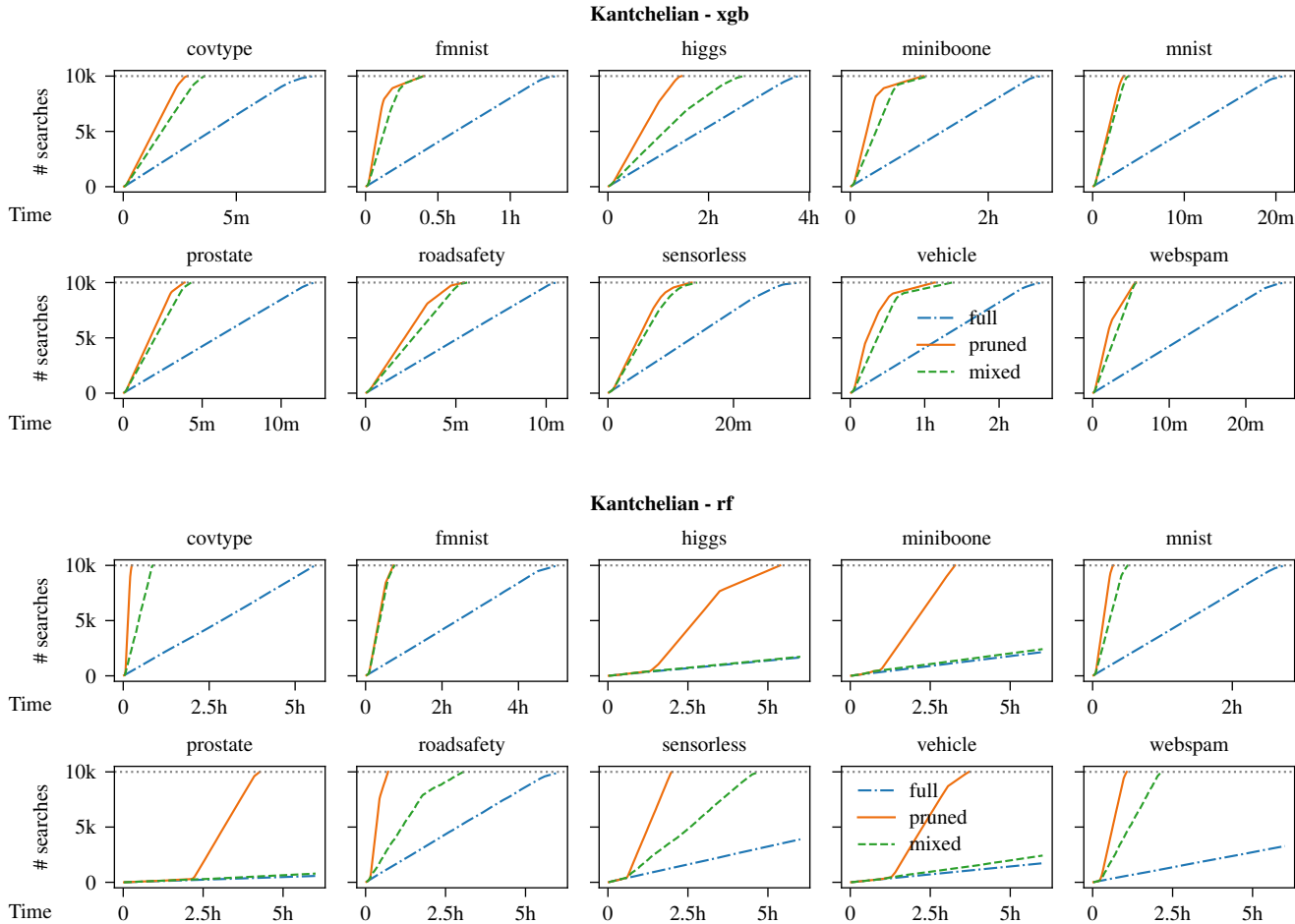


Figure 6. Run times to generate adversarial examples for 10 000 test examples for the three presented settings (*full*, *pruned* and *mixed*), using *kantchelian* on an XGBoost/random forest ensemble, averaged over 5 folds.

Figure 8 shows a large set of adversarial examples generated for a *mnist* digit using *kantchelian* and *veritas*. For each attack, we plot the base example x and the two adversarial examples generated with the *full* and the *pruned* setting.

D.1. Empirical Robustness

Table 8 shows the average empirical robustness for all experiments for the *full*, *pruned* and *mixed* settings. *Empirical robustness* is defined as the average distance to the nearest adversarial example for each x in our test set. We use adversarial examples generated with the experiments presented in Section 4.2.

The objective of the *kantchelian* attack is to find the closest adversarial example. Given that the method is exact, the *full* setting returns the optimal solution. The *pruned* search works with a restricted feature set, thus it might not be able to find the closest adversarial example, if that requires

altering features not included in the selected feature subset. As a consequence, the *empirical robustness* values for the *pruned* and *mixed* search are overestimates of the true value given by the *full* setting.

Unlike *kantchelian*, *veritas* does not try to find the closest adversarial example. Instead, it maximizes the confidence that the ensemble assigns to the incorrect label. In this case, there is little difference in the empirical robustness values among all considered settings, with the *pruned* and *mixed* settings typically managing to even lower the distance to the base example.

D.2. Change in Predicted Probability for Adversarial Examples

veritas tries to generate an adversarial example such that the ensemble assigns as high a probability as possible to the incorrect label. Hence, a natural empirical measure

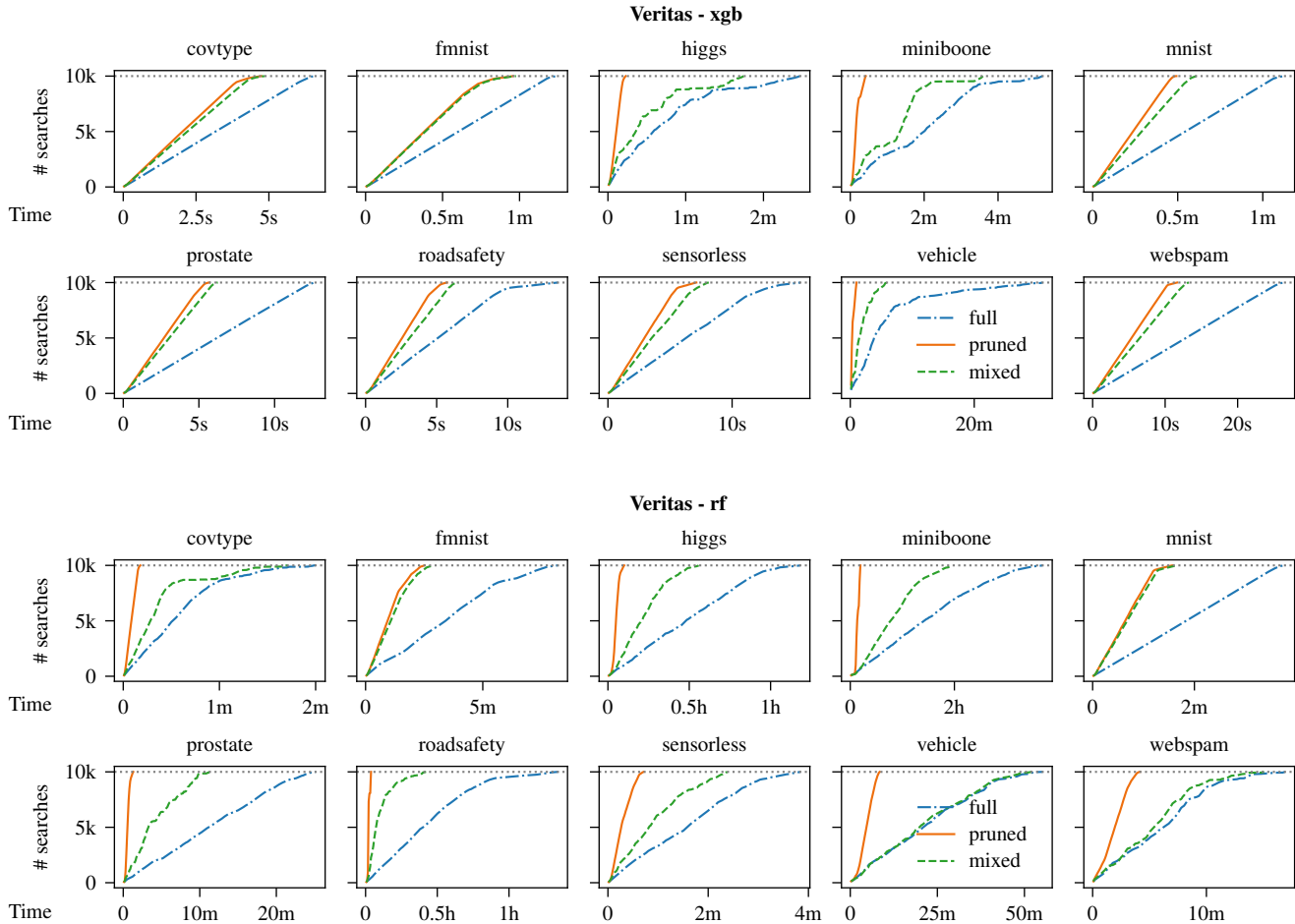


Figure 7. Run times to generate adversarial examples for 10 000 test examples for the three presented settings (*full*, *pruned* and *mixed*), using *veritas* on an XGBoost/random forest ensemble, averaged over 5 folds.

for the quality of the examples generated is to compare the difference in the ensembles probabilistic predictions for the adversarial examples generated by each approach. Namely, we compute $T(\tilde{x}) - T(\tilde{x}')$ where \tilde{x} is generated by the full search, \tilde{x}' is generated by the *pruned* (*mixed*) search, and (in an abuse of notation) $T(x)$ returns the probability an example belongs to most likely class.

Table 9 shows the average differences in predicted probability between *full* and *pruned/mixed* adversarial examples.

Using *kantchelian*, adversarial examples generated with our approaches are assigned very similar probabilities to those generated with the *full* search. In *veritas*, differences are typically higher, as the model output is directly optimized.

E. Expanded Related Work

Adversarial examples have been theoretically studied and defined in multiple different ways (Diochnos et al., 2018; Gourdeau et al., 2021). More specifically, Ilyas et al. showed how certain features in a dataset might be fragile and thus naturally lead to adversarial examples (Ilyas et al., 2019). Approaches to reason about learned tree ensembles have received substantial interest in recent years. These include algorithms for performing evasion attacks (Kantchelian et al., 2016; Einziger et al., 2019) (i.e., generate adversarial examples), perform robustness checking (Chen et al., 2019b), and verify that the ensembles satisfy certain criteria (Devos et al., 2021b;a; Ranzato & Zanella, 2020; Törnblom & Nadjm-Tehrani, 2020). Kantchelian et al. (Kantchelian et al., 2016) were the first to show that, just like neural networks, tree ensembles are susceptible to evasion attacks. Their MILP formulation is still the most frequently used

Table 6. Average run times (with standard deviations) to verify 10000 test examples using *kantchelian/veritas* on an XG-Boost/Random forest ensemble for all three approaches: *full*, *pruned* and *mixed*.

Kantchelian, XGBoost			
	<i>full</i>	<i>pruned</i>	<i>mixed</i>
covtype	7.7m ± 33.4s	2.6m ± 10.9s	3.4m ± 14.5s
fmnist	1.3h ± 2.7m	11.3m ± 6.5m	15.9m ± 4.6m
higgs	3.7h ± 7.4m	1.3h ± 9.7m	2.3h ± 25.1m
miniboone	2.7h ± 4.3m	31.4m ± 16.1m	44.9m ± 11.5m
mnist	20.0m ± 45.6s	3.2m ± 12.5s	3.6m ± 12.4s
prostate	11.8m ± 18.8s	3.4m ± 24.5s	4.0m ± 15.7s
roadsafety	10.3m ± 15.7s	4.4m ± 48.4s	5.2m ± 17.0s
sensorless	27.1m ± 2.5m	9.7m ± 2.1m	11.1m ± 2.0m
vehicle	2.4h ± 6.8m	33.6m ± 18.7m	46.8m ± 17.8m
webspam	23.7m ± 1.1m	4.3m ± 1.6m	5.5m ± 9.9s

Kantchelian, RF			
	<i>full</i>	<i>pruned</i>	<i>mixed</i>
covtype	5.6h ± 1.3m	13.1m ± 1.3m	50.6m ± 1.0m
fmnist	4.8h ± 15.8m	37.7m ± 6.1m	40.3m ± 5.0m
higgs	6.0h ± 1.8s	4.4h ± 56.6m	6.0h ± 4.5s
miniboone	6.0h ± 5.3s	3.3h ± 56.5s	6.0h ± 0.7s
mnist	2.7h ± 5.0m	16.2m ± 1.2m	27.4m ± 2.6m
prostate	6.0h ± 7.9s	4.2h ± 5.0m	6.0h ± 4.2s
roadsafety	5.8h ± 13.2m	34.3m ± 7.9m	2.4h ± 38.1m
sensorless	6.0h ± 0.2s	2.0h ± 30.5s	4.6h ± 7.3m
vehicle	6.0h ± 0.9s	3.4h ± 19.7m	6.0h ± 2.5s
webspam	6.0h ± 2.8s	1.0h ± 2.7m	2.1h ± 3.8m

Veritas, XGBoost			
	<i>full</i>	<i>pruned</i>	<i>mixed</i>
covtype	6.4s ± 0.2s	4.1s ± 0.3s	4.4s ± 0.2s
fmnist	1.2m ± 1.7s	46.3s ± 6.6s	47.2s ± 6.8s
higgs	1.4m ± 32.6s	11.6s ± 1.2s	58.0s ± 24.2s
miniboone	3.7m ± 49.4s	14.7s ± 5.2s	2.2m ± 42.0s
mnist	1.1m ± 1.8s	28.2s ± 0.8s	34.5s ± 1.7s
prostate	12.4s ± 0.2s	5.3s ± 0.3s	6.0s ± 0.2s
roadsafety	10.4s ± 1.6s	5.0s ± 0.5s	6.2s ± 0.2s
sensorless	12.9s ± 1.6s	5.8s ± 0.7s	7.2s ± 0.7s
vehicle	12.0m ± 9.7m	36.2s ± 18.6s	3.2m ± 1.6m
webspam	25.8s ± 0.6s	10.6s ± 0.5s	12.8s ± 0.5s

Veritas, RF			
	<i>full</i>	<i>pruned</i>	<i>mixed</i>
covtype	1.1m ± 27.2s	9.6s ± 0.5s	42.6s ± 29.9s
fmnist	6.9m ± 1.1m	1.9m ± 27.6s	2.2m ± 30.6s
higgs	59.8m ± 6.7m	4.4m ± 54.0s	25.1m ± 5.4m
miniboone	3.0h ± 37.1m	9.3m ± 1.7m	1.5h ± 19.2m
mnist	3.7m ± 5.2s	1.3m ± 8.6s	1.4m ± 9.0s
prostate	23.0m ± 2.0m	54.8s ± 12.1s	8.7m ± 2.1m
roadsafety	52.2m ± 15.9m	1.5m ± 22.2s	11.5m ± 7.3m
sensorless	3.0m ± 31.8s	32.9s ± 8.8s	1.7m ± 30.7s
vehicle	43.6m ± 10.1m	7.5m ± 51.5s	42.1m ± 10.4m
webspam	12.5m ± 2.8m	3.5m ± 27.6s	11.0m ± 2.8m

Table 7. Average fraction of timeouts incurred when verifying 10000 test examples using *kantchelian/veritas* on XG-Boost/Random forest for all three approaches: *full*, *pruned* and *mixed*.

Kantchelian, XGBoost			
	<i>full</i>	<i>pruned</i>	<i>mixed</i>
covtype	0%	0%	0%
fmnist	0%	<1%	0%
higgs	0%	13.2%	0%
miniboone	0%	<1%	0%
mnist	0%	0%	0%
prostate	0%	0%	0%
roadsafety	0%	0%	0%
sensorless	0%	<1%	0%
vehicle	0%	<1%	0%
webspam	0%	0%	0%

Kantchelian, RF			
	<i>full</i>	<i>pruned</i>	<i>mixed</i>
covtype	0%	<1%	0%
fmnist	0%	<1%	0%
higgs	<1%	69.6%	<1%
miniboone	0%	59.8%	0%
mnist	<1%	0%	0%
prostate	<1%	43.5%	<1%
roadsafety	0%	2.4%	0%
sensorless	0%	9.3%	0%
vehicle	0%	38.4%	0%
webspam	0%	<1%	0%

Veritas, XGBoost			
	<i>full</i>	<i>pruned</i>	<i>mixed</i>
covtype	0%	0%	0%
fmnist	0%	<1%	0%
higgs	0%	0%	0%
miniboone	<1%	0%	<1%
mnist	0%	0%	0%
prostate	0%	0%	0%
roadsafety	0%	0%	0%
sensorless	0%	<1%	0%
vehicle	<1%	<1%	<1%
webspam	0%	0%	0%

Veritas, RF			
	<i>full</i>	<i>pruned</i>	<i>mixed</i>
covtype	0%	0%	0%
fmnist	<1%	4.3%	0%
higgs	<1%	5.2%	<1%
miniboone	<1%	2.7%	<1%
mnist	0%	1.5%	0%
prostate	<1%	<1%	<1%
roadsafety	<1%	<1%	<1%
sensorless	<1%	<1%	<1%
vehicle	<1%	26.9%	<1%
webspam	<1%	10.6%	<1%

Table 8. Average empirical robustness (i.e., distance to the closest adversarial example) for the *full*, *mixed* and *pruned* methods using *kantchelian/veritas* attacks on XGBoost/RF ensembles.

Kantchelian, XGBoost			
	<i>full</i>	<i>pruned</i>	<i>mixed</i>
covtype	0.016 ± 0.001	0.036 ± 0.0	0.037 ± 0.0
fmnist	0.031 ± 0.003	0.071 ± 0.011	0.07 ± 0.01
higgs	0.011 ± 0.0	0.015 ± 0.001	0.015 ± 0.001
miniboone	0.023 ± 0.0	0.031 ± 0.002	0.033 ± 0.003
mnist	0.008 ± 0.001	0.03 ± 0.006	0.029 ± 0.005
prostate	0.02 ± 0.0	0.037 ± 0.002	0.039 ± 0.002
roadsafety	0.005 ± 0.0	0.013 ± 0.002	0.013 ± 0.002
sensorless	0.009 ± 0.0	0.014 ± 0.001	0.015 ± 0.001
vehicle	0.016 ± 0.0	0.038 ± 0.011	0.037 ± 0.009
webspam	0.002 ± 0.0	0.005 ± 0.002	0.005 ± 0.002
Kantchelian, RF			
	<i>full</i>	<i>pruned</i>	<i>mixed</i>
covtype	0.076 ± 0.0	0.089 ± 0.0	0.093 ± 0.0
fmnist	0.018 ± 0.001	0.039 ± 0.003	0.039 ± 0.002
higgs	0.016 ± 0.0	0.016 ± 0.005	0.017 ± 0.001
miniboone	0.027 ± 0.001	0.035 ± 0.0	0.03 ± 0.001
mnist	0.006 ± 0.0	0.035 ± 0.002	0.034 ± 0.003
prostate	0.048 ± 0.001	0.074 ± 0.0	0.067 ± 0.001
roadsafety	0.019 ± 0.001	0.023 ± 0.0	0.026 ± 0.0
sensorless	0.014 ± 0.0	0.022 ± 0.001	0.022 ± 0.001
vehicle	0.016 ± 0.0	0.025 ± 0.004	0.022 ± 0.001
webspam	0.003 ± 0.0	0.006 ± 0.0	0.007 ± 0.0
Veritas, XGBoost			
	<i>full</i>	<i>pruned</i>	<i>mixed</i>
covtype	0.094 ± 0.0	0.088 ± 0.002	0.089 ± 0.002
fmnist	0.291 ± 0.002	0.282 ± 0.005	0.282 ± 0.005
higgs	0.074 ± 0.001	0.069 ± 0.001	0.069 ± 0.001
miniboone	0.077 ± 0.0	0.075 ± 0.0	0.076 ± 0.0
mnist	0.291 ± 0.001	0.265 ± 0.011	0.268 ± 0.01
prostate	0.097 ± 0.0	0.095 ± 0.001	0.095 ± 0.0
roadsafety	0.057 ± 0.0	0.056 ± 0.001	0.056 ± 0.001
sensorless	0.056 ± 0.0	0.052 ± 0.002	0.052 ± 0.002
vehicle	0.14 ± 0.001	0.133 ± 0.003	0.134 ± 0.002
webspam	0.039 ± 0.0	0.035 ± 0.002	0.035 ± 0.001
Veritas, RF			
	<i>full</i>	<i>pruned</i>	<i>mixed</i>
covtype	0.271 ± 0.001	0.24 ± 0.006	0.243 ± 0.006
fmnist	0.294 ± 0.001	0.282 ± 0.004	0.283 ± 0.003
higgs	0.072 ± 0.0	0.07 ± 0.001	0.07 ± 0.0
miniboone	0.078 ± 0.0	0.077 ± 0.0	0.077 ± 0.0
mnist	0.29 ± 0.001	0.275 ± 0.005	0.276 ± 0.005
prostate	0.194 ± 0.0	0.186 ± 0.001	0.187 ± 0.001
roadsafety	0.11 ± 0.0	0.099 ± 0.005	0.1 ± 0.004
sensorless	0.112 ± 0.0	0.103 ± 0.003	0.104 ± 0.003
vehicle	0.139 ± 0.001	0.132 ± 0.002	0.136 ± 0.001
webspam	0.058 ± 0.0	0.053 ± 0.001	0.054 ± 0.001

amples. Other notable methods for adversarial example generation are SMT-based systems (Einzigler et al., 2019; Devos et al., 2021b). These approaches propose varying ways to encode a tree ensemble in a set of logical formulas using the primitives from Satisfiability Modulo Theories (SMT). While the formulation of an ensemble in SMT is very elegant, it tends to perform worse than MILP in practice.

Because MILP and SMT are exact approaches,⁷ they search for the optimal answer which in certain cases can be difficult (i.e., time consuming) to find. Often an approximate answer will be sufficient and several approximate methods have been proposed that are specifically tailored to tree ensembles. Chen et al. proposed a K -partite graph representation in which a max-clique corresponds to a specific output of the ensemble (Chen et al., 2019b; Wang et al., 2020). They introduced a fast method to approximately evaluate robustness, but it cannot generate concrete adversarial examples. Devos et al. further improved upon this work by proposing a heuristic search procedure in this graph which is capable of finding concrete adversarial examples very effectively (Devos et al., 2021a). Zhang et al. propose a method based on a greedy discrete search through the space of leaves specifically optimized for fast adversarial example generation (Zhang et al., 2020).

Another line of work focuses on making tree ensembles more robust. There are multiple approaches: adding generated adversarial examples to the training data (model hardening) (Kantchelian et al., 2016), modifying the splitting procedure (Chen et al., 2019a; Calzavara et al., 2020; Vos & Verwer, 2021), using the framework of optimal decision trees to encode robustness constraints (Vos & Verwer, 2022a), re-labeling and pruning the leaves of the trees (Vos & Verwer, 2022b), simplifying the base learner (Andriushchenko & Hein, 2019) and using a robust 0/1 loss (Guo et al., 2022). Gaining further insights into how evasion attacks target tree ensembles, like those contained in this paper, may inspire novel ways to improve the robustness of learners.

method to check robustness and generate adversarial ex-

⁷MILP is technically anytime, but the approximate solutions are not useful in practice for this problem setting, see (Devos et al., 2021a).

Table 9. Average difference in predicted probability between an adversarial example generated with the *full* setting and an adversarial example generated with the *pruned/mixed* setting, for the same base example.

	Kantchelian XGB		Kantchelian RF		Veritas XGB		Veritas RF	
	<i>pruned</i>	<i>mixed</i>	<i>pruned</i>	<i>mixed</i>	<i>pruned</i>	<i>mixed</i>	<i>pruned</i>	<i>mixed</i>
covtype	0.097	0.090	0.036	0.032	0.106	0.100	0.062	0.056
fmnist	0.018	0.017	0.045	0.045	0.319	0.314	0.376	0.341
higgs	0.010	0.008	0.016	0.006	0.094	0.090	0.053	0.046
miniboone	0.014	0.013	0.033	0.014	0.135	0.124	0.086	0.075
mnist	0.109	0.107	0.045	0.041	0.172	0.154	0.29	0.276
prostate	0.026	0.024	0.034	0.026	0.231	0.213	0.230	0.206
roadsafety	0.129	0.12	0.023	0.020	0.178	0.160	0.082	0.075
sensorless	0.058	0.052	0.053	0.045	0.122	0.110	0.148	0.133
vehicle	0.013	0.012	0.024	0.014	0.200	0.175	0.153	0.101
webspam	0.047	0.044	0.032	0.031	0.273	0.245	0.262	0.229

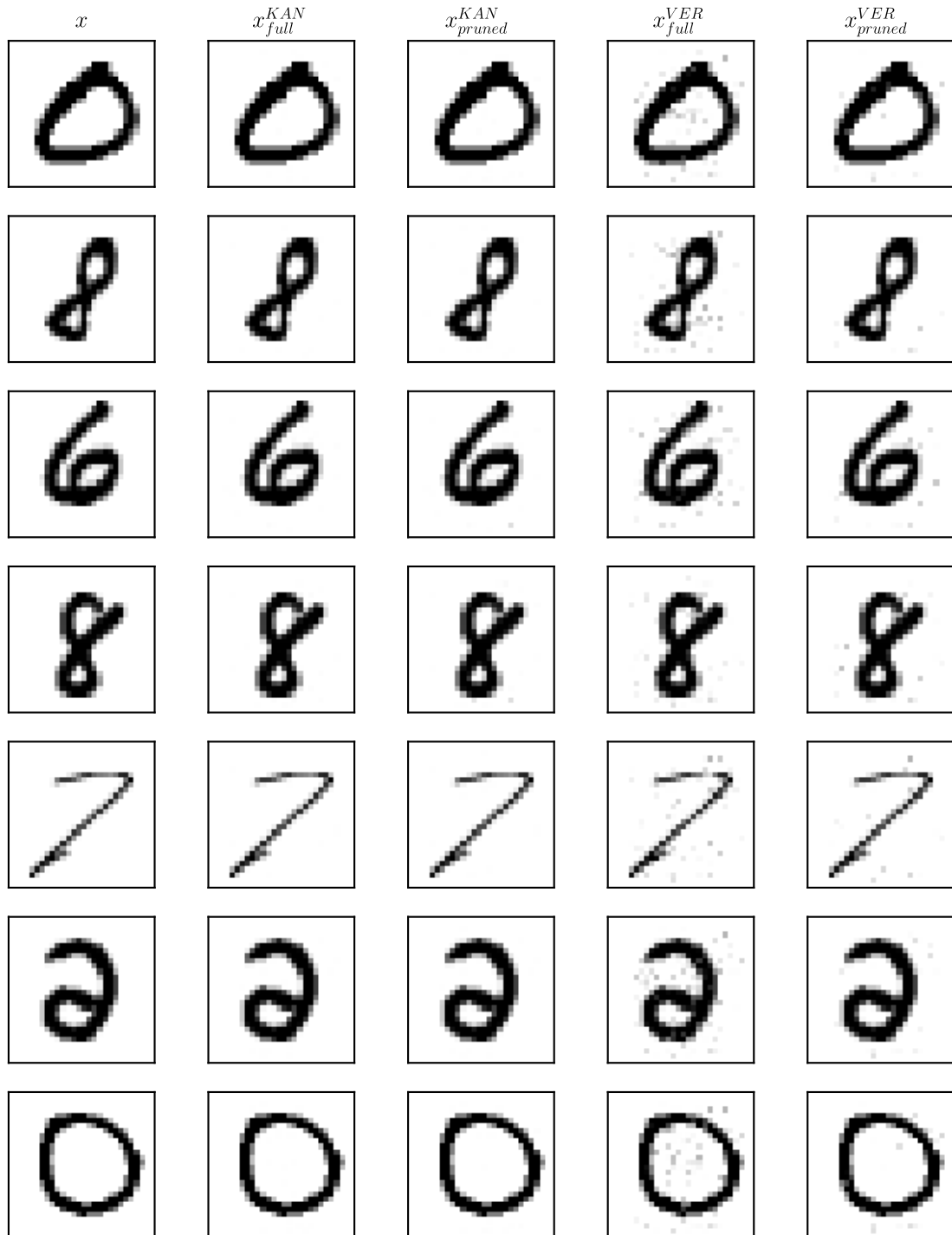


Figure 8. Adversarial examples generated for *mnist* with both attacks (*kantchelian* and *veritas*) to show the quality of generated examples.